J. exp. Biol. ***192****, 45–59 (1994)*
Printed in Great Britain © The Company of Biologists Limited 1994

STUDIES OF TROPICAL TUNA SWIMMING PERFORMANCE IN A LARGE WATER TUNNEL

III. KINEMATICS

HEIDI DEWAR AND JEFFREY B. GRAHAM*

Center for Marine Biotechnology and Biomedicine and the Marine Biology Research Division, Scripps Institution of Oceanography, 0204 La Jolla, CA 92093–0204, USA

Accepted 23 February 1994

Summary

Yellowfin tuna (*Thunnus albacares*) swimming kinematics was studied in a large water tunnel at controlled swimming velocities (U). Quantified kinematic variables included the tail-beat frequency, stride length (l), caudal amplitude, yaw, the propulsive wavelength, the speed of the propulsive wave (C) and the sweepback angle of the pectoral fins. In general, all variables, except the propulsive wavelength and consequently C, are comparable to values determined for other teleosts. The propulsive wavelength for the tunas (1.23–1.29L, where L is fork length) is 30–60 % longer than in other cruise-adapted teleosts such as salmonids. The resulting thunniform swimming mode and the morphological and anatomical adaptations associated with the long propulsive wavelength (e.g. fusiform body shape, rigid vertebral column) act to minimize anterior resistance and maximize caudal thrust. The long propulsive wavelength also increases the maximum l which, in concert with the elevated muscle temperatures of tunas, increases their maximum swimming velocity.

Introduction

In a now classic work, Gray (1933) employed a two-wave system to describe the body movements of swimming fish. The first wave traces the caudal fin through a propulsive cycle and has a characteristic amplitude, frequency or tail-beat frequency (*TBF*), wave velocity [the same as the swimming speed (U)] and wavelength [which equals the stride length (l) or distance travelled per tail-beat]. The second, or propulsive, wave results from the progression of muscular contraction from the head to the tail. It also has a velocity (C), a frequency (also *TBF*), a characteristic propulsive wavelength (λ) and an

*To whom reprint requests should be addressed.

Key words: tuna, *Thunnus albacares*, locomotion, swimming mechanics, kinematics, thunniform.

amplitude (which varies along the body). For both waves, velocity=wavelength×*TBF* and defining both in terms of *TBF* provides the relationship:

$$U \times l^{-1} = C \times \lambda^{-1},$$

and thus

$$U \times C^{-1} = l \times \lambda^{-1}.$$

Because $C>U$ is required for thrust generation (Gray, 1933; Webb, 1975), it follows that l can only approach, but never exceed, the propulsive wavelength during steady motion.

The wave characteristics described above classify the broad spectrum of fish swimming styles and indicate the relative importance of the body segments and the paired and medial fins in thrust generation (Webb, 1975; summarised by Lindsey, 1978). In the anguilliform mode, for example, the propulsive wavelength is short and the amplitude along the entire body relatively large, which indicates that the body segments are primarily responsible for thrust generation (Gray, 1933). At the other extreme, the thunniform swimming mode employed by tunas has a long propulsive wavelength and the majority of lateral motion occurs caudally. The high-aspect-ratio lunate tail is the primary propulsor and anterior lateral movements (e.g. yaw) contribute only to drag.

Although thunniform swimming has been categorized in general terms (Fierstine and Walters, 1968; Webb, 1975; Magnuson, 1978), obtaining a more complete understanding of tuna swimming mechanics has been complicated by the limited opportunities for close examination of stably swimming fish. Nevertheless, unique muscular and biomechanical characteristics have been invoked to explain the means by which tuna attain high burst velocities (Brill and Dizon, 1979; Wardle and Videler, 1980). Related questions concerning thrust generation and swimming performance at sustained speeds have been complicated by the unavailability of a detailed description of tuna swimming kinematics. The previous inability to control *U* has also limited studies.

Much of the current information about the kinematic variables associated with the two-wave system discussed above (beyond the relatively simple measurements of *TBF*) is derived from a study by Fierstine and Walters (1968). These investigators examined one tail-beat cycle at five speeds for kawakawa (*Euthynnus affinis*) swimming in large circular tanks. Other important studies by Magnuson have examined the components of drag and thrust, the elements of tuna caudal movements, the actions of the finlets, the role of the pectoral fins in developing lift and, concurrently, the minimum swimming speed (U_{min}) required to maintain hydrostatic equilibrium (Magnuson, 1970, 1973, 1978). The most complete summary of the data available on scombrid swimming mechanics is provided in the paper of Magnuson (1978).

This paper reports observations of tuna swimming kinematics carried out on fish swimming stably at controlled *U* and has three primary goals. First, to establish the best estimates for the basic kinematic variables for tunas and to compare these with values determined for other teleosts. Second, to examine the functional significance of the anatomical and morphological adaptations of tunas for swimming. Third, to estimate the maximum swimming speed of tunas on the basis of swimming kinematics and muscle mechanics.

Materials and methods

Kinematic observations were made on yellowfin tuna (*Thunnus albacares*) swimming at controlled U and ambient temperatures (T_a=24–28 °C) in a large (3000 l) recirculating water tunnel (Graham *et al.* 1990). Details about the water tunnel and the methods for handling tunas are reported in Dewar and Graham (1994).

Determination of kinematic variables

For fish that were swimming steadily at a constant U, *TBF* was determined using a stopwatch to record the time required for 20 tail-beats. In general, five replicate determinations were made 3–4 times at each experimental U. l was then calculated from the relationship between *TBF* and U. Because this method is relatively simple, the sample size for *TBF* and l is greater than for the other variables. Also, data were recorded for a larger number of fish.

Video recordings of stably swimming fish were digitized to quantify the caudal amplitude, yaw, C, the propulsive wavelength and the pectoral-fin sweepback angle. A mirror mounted at a 45 ° angle over the transparent top of the water tunnel's working section made it possible to record the fish's dorsal profile. Video recordings were made over a 2–5 min period at each experimental U using a Sony FX-800 video 8 camera. Shutter speeds up to 1/200 s were used, depending on U and the available lighting. While it would have been ideal always to record the movements of the entire body, this was often precluded by the requirement not to disturb the fish by uncovering the upstream region of the working section.

Video analysis

Selection of video segments for digital analysis (2–5 min videos) was based on several criteria. Sections were chosen only when the fish was away from both channel walls and its position, both parallel and perpendicular to flow, remained constant. Also, only segments in which the view was from precisely overhead were analyzed. The chosen segments spanned a minimum of 2 s and at least five tail-beats.

Prior to digitization, selected video 8 segments were transferred onto VHS format and a time code incorporated to label each frame numerically. A Panasonic (model no. AG-1960) and a JVC (model no. HR-S26700U) VCR enabled advancement of the video images frame by frame (VHS, 30 frames s^{-1}) or field by field (Panasonic, 60 fields s^{-1}, used when U>100 cm s^{-1}). A frame grabber transferred the selected video images to the computer monitor, where the Cartesian coordinates for specified parts of the fish's body were determined. The same points on the fish were digitized in successive images to permit examination of their temporal progression.

Up to five points on the tuna's body were digitized in each video image, depending on the extent of the body visible. Ideally, the tip of the snout, the base of the pectoral fins, a point close to the second dorsal fin, and both the proximal base and distal tips of the caudal fin were digitized. When visible, the second dorsal fin served as a natural marker; otherwise, the mid-point of the body positioned over a perpendicular grid line was used. For a 44 cm yellowfin swimming at 46 cm s^{-1}, the outline of the entire body was digitized through one propulsive cycle.

Results

Tail-beat frequency and stride length

Fig. 1 shows all *TBF* data collected for the three size classes of yellowfin tuna as a function of *U*. Data for the size classes [separated on the basis of fork length (*L*)], together with the least-squares regression lines, are given in Table 1. Regression analyses indicate a significant increase in *TBF* with *U*. Examination of the differences in slope suggests an inverse relationship with *L*. The slope for the largest group (53 cm *L*) is significantly less than for the 32 cm and 42 cm groups, and the elevations between the two smaller groups differ significantly ($P<0.05$, ANCOVA).

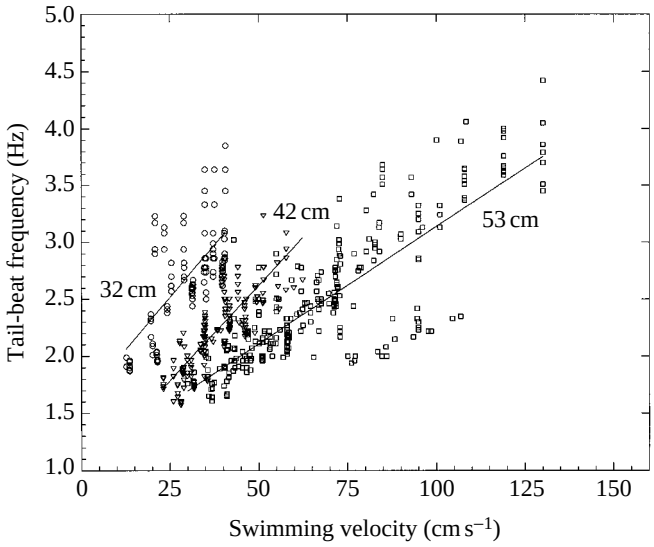

Fig. 1. Relationship between tail-beat frequency (*TBF*) and swimming velocity (*U*) for the three size classes of yellowfin tuna; 32 cm (circles), 42 cm (triangles) and 53 cm (squares). The least-squares regression line calculated for each size class is shown (see Table 1).

Table 1. *Summary of* U/TBF *regression variables for the three size classes of yellowfin (*Thunnus albacares*)*

L (cm)	*N*	Slope	Intercept	r^2
32 (±0.2)	130	0.037 (±0.0034)	1.60 (±0.32)	0.47
42 (±1.6)	234	0.033 (±0.0015)	0.95 (±0.19)	0.69
53 (±3.0)	301	0.021 (±0.0008)	1.08 (±0.33)	0.68

L, fork length; *TBF*, tail-beat frequency; *U*, swimming velocity; *N*, number of fish; r^2, regression coefficient.

Values are mean ± S.D. for *L* and mean ± S.E.M. (for slope and intercept).

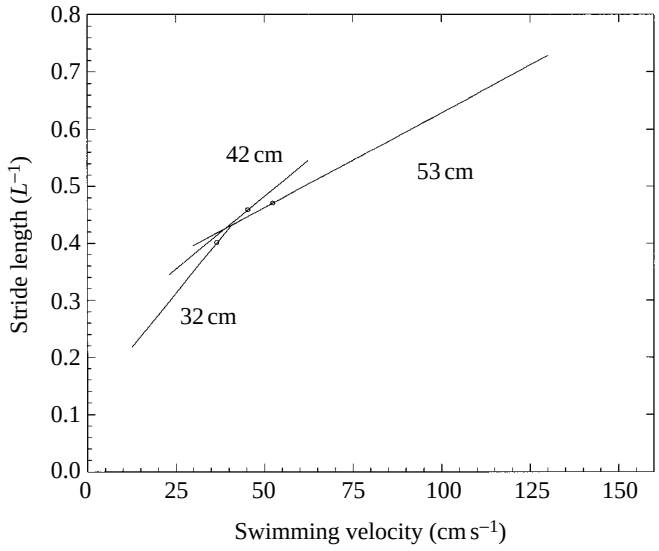

Fig. 2. Stride length, given in units of fork length (L^{-1}), as a function of U for the three size classes of yellowfin tuna. The small circles represent U_{min} (see text).

Regression analysis also demonstrates that l is directly dependent on U for all three groups (Fig. 2). (It should be noted that, although the data are examined using linear regression analysis, at higher U the l will probably reach a maximum as it approaches the value for the propulsive wavelength.) Comparison of the three size classes of yellowfin shows an inverse relationship between slope and L. Also, the percentage of the data range occurring below U_{min} is greatest for the smaller yellowfin. [Note that l and the other kinematic variables that change with size are reported as length-specific values. For example, if the distance travelled per tail beat is 30 cm for a 50 cm tuna, l is $0.6L^{-1}$ (30 cm/50 cm).]

Digital analysis of swimming mechanics

Fig. 3A shows the dorsal view of the lateral undulations of a 44 cm yellowfin tuna at 1/15 s intervals through one tail-beat cycle (U=46 cm s^{-1}). The same images are superimposed in Fig. 3B. Fig. 3C shows the individual waves obtained by following the lateral excursion of the four points on the body (Fig. 3A) through two cycles. This formed the basis for determination of all kinematic variables. Digital analyses conducted on all fish are summarised in Table 2, which shows the mean L, the number of individual fish and video segments examined, as well as the mean and range of U used for each yellowfin size group.

Caudal amplitude and yaw

From the wave patterns shown in Fig. 3C it is possible to determine the maximum excursion of points 1–4. (The base of the pectoral fins is not included because without a marker it was not possible to select a consistent point in successive frames.) The caudal

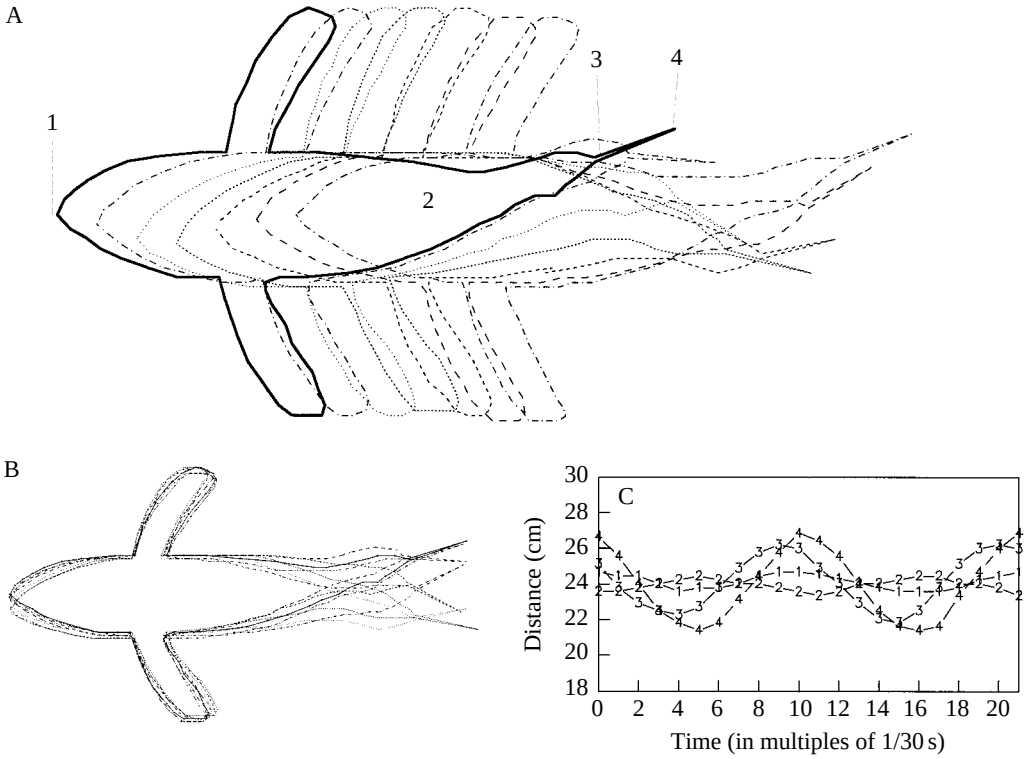

Fig. 3. (A) Successive dorsal profiles of a 44 cm yellowfin tuna swimming at 46 cm s^{-1}, determined at 1/15 s intervals. Also indicated are the four points digitized. (B) Images from A overlain. (C) The lateral excursion of the four points indicated in A as a function of time.

Table 2. *Summary of digital analyses carried out on the three size groups of yellowfin (*Thunnus albacares*)*

L (cm)	Number of fish	Video segments	Mean *U* (cm s^{-1})	*U* range (cm s^{-1})
32 (±0.5)	4	11	31	17–43
42 (±1.6)	5	17	48	26–74
48 (±2.2)	5	27	87	27–150

L, fork length; *U*, swimming velocity.
Values in parentheses are S.D.

amplitude is the distance between the lateral extremes of wave no. 4. Least-squares regression analyses for each size class and on the combined data for all fish indicate no effect of *U* on amplitude, which ranges between 0.17 and 0.20L^{-1} (Table 3). The apparent

Table 3. *Summary of the mean* L, U, *length-specific amplitude and yaw for the three size classes of yellowfin (*Thunnus albacares*)*

L (cm)	*U* (cm s^{-1})	Amplitude (*L*$^{-1}$)	*U* (cm s^{-1})	Yaw (*L*$^{-1}$)
32 (±0.5)	31 (±2.4)	0.20 (±0.010)	32 (±3.8)	0.038 (±0.0013)
42 (±1.6)	48 (±3.1)	0.18 (±0.007)	40 (±2.8)	0.043 (±0.0017)
48 (±2.2)	87 (±6.7)	0.17 (±0.003)	100 (±6.5)	0.028 (±0.0007)

L, fork length; *U*, swimming velocity.
Values for *L* and *U* are mean ± S.D.; values for amplitude and yaw are ±S.E.M.

decrease in amplitude with body size is not significant (P<0.05; non-parametric rank sum test).

Table 3 also shows the mean yaw (amplitude of wave no. 1; Fig. 3C) for each size class of yellowfin. Least-squares regression analysis on all yellowfin data indicates that yaw decreases significantly with U as described by:

$$\text{yaw}\ (L^{-1}) = 0.047 - 0.0002U\ (\text{cm s}^{-1})\ (N=30,\ r^2=0.67)\,.$$

Propulsive wave velocity

The velocity of the propulsive wave (C) is also determined from Fig. 3C by measuring the time between peaks in successive body segments that are separated by a known distance. When possible, C was determined over the entire body; however, when only the caudal region was visible, the distance from second dorsal fin to the tip of the caudal fin was used. The mean C, calculated for the same fish over the whole body and over just the caudal region, did not differ (P<0.05; non-parametric rank sum test). Measurement of C enables calculation of the U:C ratio, and least-squares regression analysis on all yellowfin data indicates that $U \times C^{-1}$ increases significantly with U, as described by:

$$U \times C^{-1} = 0.26 + 0.0021U\ (\text{cm s}^{-1})\ (N=30,\ r^2=0.84).$$

Propulsive wavelength

Quantification of C also permits estimation of the propulsive wavelength (λ) ($\lambda = C \times TBF^{-1}$). The propulsive wavelength is independent of U and the mean values (Table 4) range from 1.23 to 1.29L^{-1}. The slight differences between the three groups are not significant (P<0.05, non-parametric rank sum test).

Pectoral-fin sweepback angle

To avoid potential complications imposed by the pivoting of the pectoral fins (apparent in Fig. 3B), the sweepback angle was measured (Fig. 4) at the lateral extremes and at the mid-point of the caudal propulsive cycle. The means of these three values, determined for

Table 4. *Summary of the mean* L, U *and length-specific propulsive wavelength for the three size classes of yellowfin (*Thunnus albacares*)*

L (cm)	*U* (cm s^{-1})	Wavelength (L^{-1})
32 (±0.5)	33 (±5.0)	1.29 (±0.21)
42 (±1.6)	47 (±9.8)	1.24 (±0.09)
48 (±2.2)	92 (±33)	1.23 (±0.17)

L, fork length; *U*, swimming velocity.
Values for *L* are mean ± S.D.; values for *U* and wavelength are ±S.E.M.

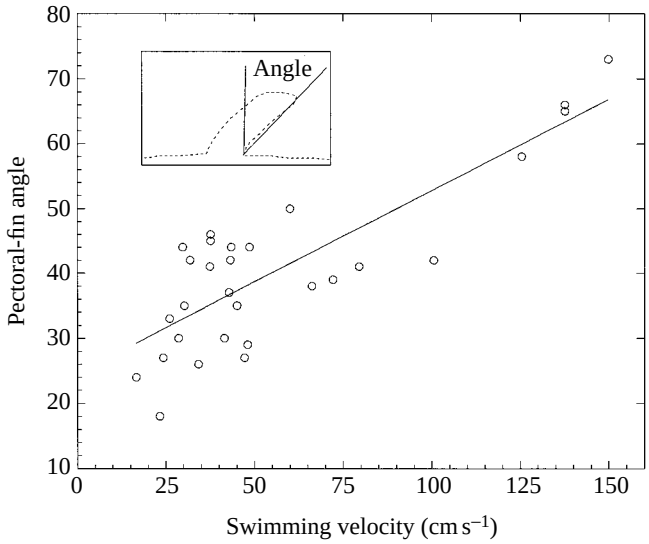

Fig. 4. Yellowfin pectoral-fin sweepback angle as a function of *U* (cm s^{-1}). The line represents the least-squares regression equation (see text).

all yellowfin, are plotted as a function of *U* in Fig. 4. Least-squares regression analysis on all data indicates that the sweepback angle increases significantly with *U* [sweepback angle=24+0.28*U* (cm s^{-1}) (*N*=30, r^2=0.69)].

Discussion

Swimming mechanics

The movements of a swimming fish represent the cumulative interactions of its locomotor infrastructure and the physical forces imposed by the aquatic medium.

Quantification of movement can therefore provide insights into tuna swimming mechanics and the functional significance of the numerous morphological, muscular and skeletal characteristics that are considered to enhance swimming.

The localization and distribution of the locomotor muscle of tunas differs from that of other teleosts. Coincident with the strongly fusiform shape is the anterior localization of the tuna's muscle mass and the insertion of the myotomes over a larger number of vertebrae (Nursall, 1956; Fierstine and Walters, 1968; Aleyev, 1977; Magnuson, 1978). The maximum cross-sectional area of the aerobic (red) locomotor muscle occurs at approximately 50 % *L*, in comparison to the 75 % *L* observed in many other fishes (Greer-Walker and Pull, 1975; Graham *et al.* 1983). Tuna red muscle also differs in that it lies adjacent to the backbone and not in a subcutaneous lateral wedge as in most other teleosts (Kishinouye, 1923; Carey and Teal, 1966; Graham *et al.* 1983). Although the importance of the central red muscle for endothermy is clear, the biomechanical implications of this arrangement remain to be determined. Lack of knowledge concerning the specific mechanical linkages between the propulsive musculature and the backbone, skin and caudal fin complicates this matter.

Another dominant component of force transmission and swimming mechanics is the compliance of the vertebral column. Rotation around intervertebral joints in tunas is limited by the articulation of zygapophyses (Nursall, 1956; Fierstine and Walters, 1968). Bending is thus limited primarily to the pre- and postpeduncular joints at the proximal and distal end of the caudal peduncle. The caudal peduncle itself is rigid owing to the bony lateral keels and the overlapping, recumbent neural and haemal spines (Nursall, 1956; Fierstine and Walters, 1968; Magnuson, 1978).

General description of yellowfin swimming

Fig. 3 allows examination of the undulatory movements of a yellowfin through a propulsive cycle. Although the successive profiles (Fig. 3A) give the impression of minimal anterior lateral motion, the superimposed images (Fig. 3B) illustrate considerable yaw. This becomes reduced at the base of the pectoral fins, but our analysis reveals that there is not a point of zero motion.

Although yawing occurs, most lateral motion takes place over the caudal region. Proceeding caudally from the base of the pectoral fins, the amplitude gradually increases and the envelope of lateral excursion does not extend beyond the point of maximal thickness until the caudal peduncle. Here, the dual joint system permits greater rotation, and a marked increase in amplitude occurs at the caudal tip. The pre- and postpeduncular joints and the stout ligaments are thought to focus the propulsive energy and motion generated by anterior musculature at the caudal fin (Nursall, 1956; Fierstine and Walters, 1968).

Swimming kinematics

With the exception of the propulsive wavelength (and also *C*), our analysis reveals that all kinematic variables measured for the yellowfin are similar to those of other teleosts. A comparative discussion of each variable follows.

Tail-beat frequency

For tunas, as in most fishes, *TBF* increases with *U* (Bainbridge, 1958; Hunter and

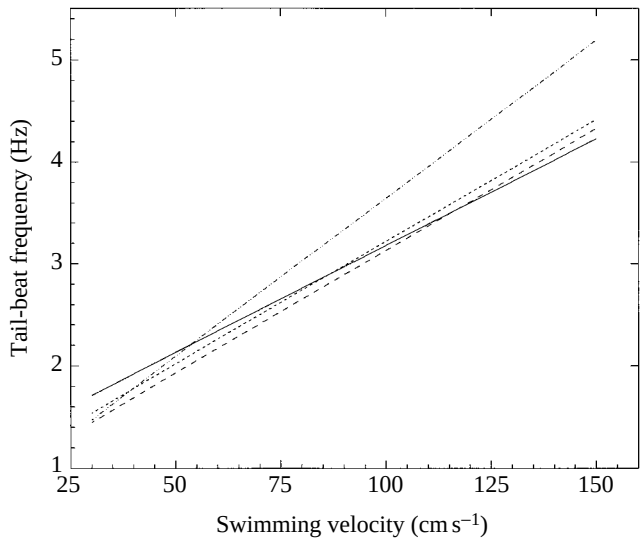

Fig. 5. Tail-beat frequency in relation to swimming velocity for the 53 cm yellowfin tuna group (solid line) and for 50 cm Pacific mackerel (dashed line), jack mackerel (dotted line) and rainbow trout (dashed and dotted line) (Hunter and Zweifel, 1971).

Zweifel, 1971; Webb, 1975; Webb *et al.* 1984). Although the range of *TBF* values is similar to that of other teleosts, our data show the slope for tunas to be less. Fig. 5 compares *TBF* data for the 53 cm yellowfin group with values determined by Hunter and Zweifel (1971) for 50 cm Pacific mackerel (*Scomber japonicus*), rainbow trout (*Oncorhynchus mykiss*) and jack mackerel (*Trachurus symmetricus*). The lower slope of the yellowfin tuna may stem from the considerable morphological adaptations for drag reduction or from adaptations affecting thrust production or propeller efficiency (discussed below).

Stride length

The functional significance of *TBF* differences is further revealed by comparisons of *l*. Determination of *l* and its dependence on *U* is important for examining sustained swimming speeds and for estimating the relationship between maximum *U* and maximum *TBF*. In previous reports for tunas, the dependence of *l* on *U* has ranged from negative to positive (Yuen, 1966; Fierstine and Walters, 1968; Graham *et al.* 1989; Wardle *et al.* 1989). Our study, and that of Fierstine and Walters (1968), demonstrates that *l* increases with *U* (Fig. 2), which agrees with data collected for a number of other teleosts (Hunter and Zweifel, 1971; Webb *et al.* 1984). The range of *l* reported here is also similar to that of other teleosts [0.6–0.8 (Bainbridge, 1958; Webb, 1975; Webb *et al.* 1984)], but the capacity of scombrids to attain a *l* higher than $0.8L^{-1}$ has been demonstrated (Wardle and He, 1988; Wardle *et al.* 1989). Our study has also revealed relatively low *l* values in smaller yellowfin (0.2–0.4; Fig. 2) at speeds below U_{min}. This may result from a decrease in swimming efficiency associated with the compensatory mechanisms employed to

increase lift. Also, drag may increase at low U because the energy loss associated with inertial recoil is inversely related to *TBF* and consequently U (Lighthill, 1977; Webb, 1988). Unlike many other fish, tunas lack an alternative mode of propulsion at low U.

Caudal amplitude

Although amplitudes determined in this study are less than the $0.21L^{-1}$ value described by Hunter and Zweifel (1971) as typical for a number of marine teleosts, they fall within the range of values ($0.13–0.21L^{-1}$) reported by other investigators (Bainbridge, 1958; Webb *et al.* 1984) and are similar to the value for giant bluefin ($0.16L^{-1}$; Wardle *et al.* 1989). Reports of values up to $0.34L^{-1}$ at a U of $8.2\,L\,s^{-1}$ (Fierstine and Walters, 1968), however, suggest that tuna are capable of greater amplitudes than measured here.

Yaw

Fish generally achieve yaw reduction through an increased body depth, which resists the anterior lateral motion resulting from recoil forces (Lighthill, 1977; Magnuson, 1978; Webb, 1988, 1992). For tunas, it has been generally held that the structural and mechanical separation of the body from the caudal fin reduces recoil (Aleyev, 1977; Lighthill, 1975; Magnuson, 1978). This diminishes the need for an increased anterior depth and permits adoption of a fusiform body shape.

Contrary to the previous descriptions of tuna swimming mechanics, the yaw for yellowfin determined in this study is comparable to values reported for other teleosts. Our range of values ($0.023–0.05L^{-1}$) is similar to the range $0.025–0.07L^{-1}$ reported by Webb (1988, 1992) for the bluegill sunfish (*Lepomis macrochirus*), rainbow trout and tiger musky (*Esox* sp.). That the yaw for the yellowfin is not greater, given the lack of typical yaw-reducing adaptations, attests to the mechanical separation of the caudal fin and body, as well as to the contribution of the second dorsal and anal fins to the reduction of recoil (Magnuson, 1978). Our results also indicate that yaw, and thus the energy loss associated with recoil, decreases with U. This is expected because yaw is inversely proportional to both *TBF* and $U\times C^{-1}$ (Lighthill, 1977; Webb, 1988, 1992).

Propulsive wave velocity

The ratio of U to C is considered to indicate swimming efficiency (Lighthill, 1975; Wu and Yates, 1978; Webb *et al.* 1984). Comparison of yellowfin and other teleosts (Fig. 6), however, shows that the $U\times C^{-1}$ ratio for the latter is approximately 40 % higher, suggesting that tunas are less efficient swimmers. This is counterintuitive to expectations and to results from energetic studies indicating that tunas are more efficient swimmers (Gooding *et al.* 1981; Graham *et al.* 1989; Dewar and Graham, 1994).

The low $U\times C^{-1}$ ratio for the yellowfin is attributable to its long propulsive wavelength, which results in a high C (C=wavelength$\times$*TBF*). Thus, even though *TBF* and l are comparable to those of other teleosts, the $U\times C^{-1}$ ratio indicates that the yellowfin is a less efficient swimmer. This suggests that for comparisons made on fish with different propulsive wavelengths, $U\times C^{-1}$ does not accurately portray efficiency. The $U\times C^{-1}$ ratio does, however, indicate performance scope (i.e. $U\times C^{-1}$ approaches 1 as U increases). Thus, the low values for tuna may only reflect the low range of test speeds used in this study in comparison with their potential swimming speeds.

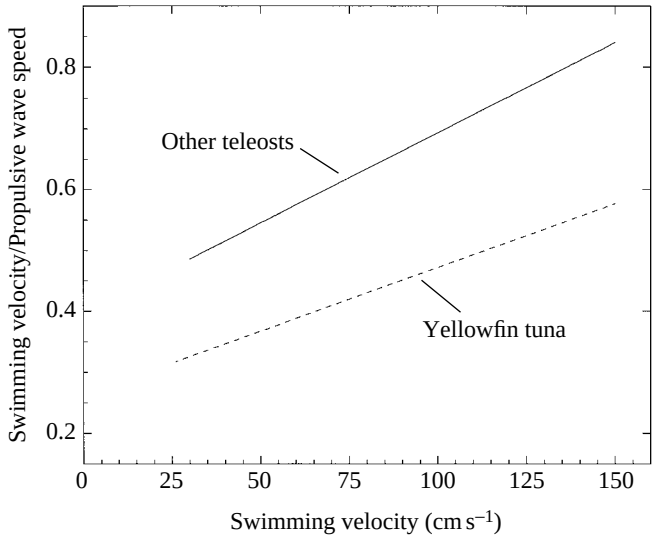

Fig. 6. $U \times C^{-1}$ as a function of U is shown for the yellowfin tuna from this study (dashed line) as well as for a number of other teleosts (solid line) (Wu and Yates, 1978).

Propulsive wavelength

As discussed above, propulsive wavelength is perhaps the most important kinematic variable. It defines swimming mode, indicates factors dominating thrust and drag, and sets the upper limit on l. Consequently, accurate assessment of this variable is essential. Previous investigators were forced to determine the propulsive wavelength from still images and the reported values range from 1 to $2L^{-1}$ (Fierstine and Walters, 1968).

Use of digital analysis enabled more precise estimation of yellowfin propulsive wavelength. Our values ($1.23–1.29L^{-1}$) exceed those of other sustained-swimming teleosts such as salmonids [$0.7–0.9L^{-1}$ (Bainbridge, 1958; Webb *et al.* 1984; Webb, 1988, 1992)]. The 30–60 % longer propulsive wavelength for the yellowfin translates directly into a greater maximum l.

A longer propulsive wavelength distinguishes yellowfin (and probably all tuna) swimming from that of other teleosts and is attributable to a suite of morphological adaptations for locomotion. Both the rigid vertebral column and the insertion of myotomes over a greater number of vertebrae should reduce regional bending and thus lengthen the propulsive wavelength. As a result, muscular force is focused on the caudal fin and not on body segments which are ineffective for thrust generation. Also, assuming that the greatest muscular cross-sectional area is primarily responsible for the portion of the tail-beat cycle where the majority of thrust is generated, a specific phase difference between the time of muscle contraction and the sweep of the caudal fin across the mid-line is required. If the distance between the muscle and the caudal fin increases, then the propulsive wavelength must also increase in order to conserve the propulsive phase relationship. The external morphology associated with the distribution of muscle (i.e. fusiform body shape) should also increase swimming efficiency by reducing drag.

Although the locomotor advantages of a long propulsive wavelength are considerable, there are also disadvantages. For a fish with one or more waves on the body, the inertial recoil forces imposed by one part of the body wave going in one direction are countered by a portion of the body going in the opposite direction (Lighthill, 1977). This may help to explain the relatively high yaw observed for yellowfin at low U.

Sweepback angle

Although the sweepback-angle equation indicates that at U=235 cm s^{-1} the pectoral fins will be completely adducted, the actual value of U is probably less; there is likely to be a point before the sweepback angle reaches 90 ˚ where the fins become ineffective for lift generation. In support of this, yellowfin swimming at 150 cm s^{-1} sporadically adducted their pectoral fins. Complete pectoral-fin adduction may result in a 23 % reduction of resistive forces; this is the estimated contribution of these fins to total drag (Magnuson, 1978). Whether energetic savings are incurred as the sweepback angle increases is difficult to determine because, although the reduction in surface area reduces friction drag, a higher U increases friction drag. Pressure and induced drag must also be considered.

Maximum swimming velocity

The maximum U (U_{max}) of a fish is directly related to its greatest attainable l and *TBF* and can be calculated as $U_{max}=l\times 2\,T^{-1}$, where T is the time (s) between nervous stimulation and the peak of muscular contraction for an unloaded muscle (Wardle, 1975; Brill and Dizon, 1979; Wardle and Videler, 1980). Examination of the components of this equation indicate that both a long l (discussed above) and a short T contribute to the tuna's high burst swimming speeds. At equivalent temperatures, the T values for tunas and other teleosts are comparable (Brill and Dizon, 1979; Johnston and Brill, 1984); however, T is reduced in tunas as a consequence of endothermy (T is inversely related to temperature).

Even though the anaerobic (white) muscle of tunas does not contribute to heat production, thermal profiles indicate that the average white muscle thermal excess (T_x=muscle temperature minus T_a) can be half that of the red muscle (Carey, 1973; Graham and Dickson, 1981). Consequently, at high U, the red muscle T_x can reach 10 ˚C and the white muscle T_x can reach 5 ˚C (Stevens and Fry, 1971). Thus, the estimated U_{max} for a 40 cm tuna at a T_a of 25 ˚C is 27 L s^{-1} [1.2/0.044; T=0.022 s at 30 ˚C (Brill and Dizon, 1979)]; this is within the range of maximum burst velocities reported for tunas (20–27 L s^{-1}; summarised by Magnuson, 1978). For comparison, the U_{max} for a similar-sized salmonid is 13 L s^{-1} [0.8/0.06; T=0.03 s at 25 ˚C (Brill and Dizon, 1979)]. Thus, both swimming mode and endothermy contribute to the high-burst swimming speeds of tunas.

We thank Drs J. R. Hunter, R. H. Rosenblatt, R. Shabetai, R. E. Shadwick and Chin Lai for commenting on drafts of this work. We also thank S. Zimmermann, P. Fields, S. Arce, C. Lowe, G. Spencer, D. Reisinger, K. Korsmeyer, R. Brill and the staff at the NMFS Kewalo Basin Research Facility for assistance. This research was supported by the US National Science Foundation (OCE-89-15927 and 91-03739). Additional funding was

received from the William H. and Mattie Wattis Harris Foundation, the Academic Rewards for College Scientists Foundation, Inc., the Maurice Massarini Charitable Trust and the SIO Tuna Endowment Fund. We thank the Southwest Fisheries Science Center NMFS for facilitating our work at the Kewalo facility.

References

ALEYEV, Y. G. (1977). *Nekton*. The Hague: Junk.

BAINBRIDGE, R. (1958). The speed of swimming fish as related to size and to the frequency and the amplitude of the tail beat. *J. exp. Biol.* **35**, 109–133.

BRILL, R. W. AND DIZON, A. E. (1979). Effect of temperature on isotonic twitch of white muscle and predicted maximum swimming speed of skipjack tuna, *Katsuwonus pelamis*. *Env. Biol. Fish.* **4**, 199–205.

CAREY, F. G. (1973). Fishes with warm bodies. *Scient. Am.* **228**, 36–44.

CAREY, F. G. AND TEAL, J. M. (1966). Heat conservation in tuna fish muscle. *Proc. natn. Acad. Sci. U.S.A.* **56**, 1464–1469.

DEWAR, H. AND GRAHAM, J. B. (1994). Studies of tropical tuna swimming performance in a large water tunnel. I. Energetics. *J. exp. Biol.* **192**, 13–31.

FIERSTINE, H. L. AND WALTERS, V. (1968). Studies in locomotion and anatomy of scombroid fishes. *Mem. S. Calif. Acad. Sci.* **6**, 1–31.

GOODING, R. M., NEILL, W. H. AND DIZON, A. E. (1981). Respiration rates and low oxygen tolerance limits in skipjack tuna, *Katsuwonus pelamis*. *Fishery Bull. Fish Wildl. Serv. U.S.* **79**, 31–48.

GRAHAM, J. B., DEWAR, H., LAI, N. C., LOWELL, W. R. AND ARCE, S. M. (1990). Aspects of shark swimming performance determined using a large water tunnel. *J. exp. Biol.* **151**, 175–192.

GRAHAM, J. B. AND DICKSON, K. A. (1981). Physiological thermoregulation in the albacore tuna (*Thunnus alalunga*). *Physiol. Zool.* **54**, 470–486.

GRAHAM, J. B., KOHERN, F. J. AND DICKSON, K. A. (1983). Distribution and relative proportions of red muscle in scombrid fishes: consequences of body size and the relationships to locomotion and endothermy. *Can. J. Zool.* **61**, 2087–2096.

GRAHAM, J. B., LOWELL, R. W., LAI, N. C. AND LAURS, R. M. (1989). O_2 tension, swimming velocity and thermal effects on the metabolic rate of the Pacific albacore, *Thunnus alalunga. Exp. Biol.* **48**, 89–94.

GRAY, J. (1933). Studies in animal locomotion. I. The movements of fish with special reference to the eel. *J. exp. Biol.* **10**, 88–104.

GREER-WALKER, M. AND PULL, G. (1975). A survey of red and white muscle in marine fishes. *Fish Biol.* **7**, 294–300.

HUNTER, J. R. AND ZWEIFEL, J. R. (1971). Swimming speed, tail beat frequency, tail beat amplitude and size in jack mackerel, *Trachurus symmetricus* and other fishes. *Fishery Bull. Fish Wildl. Serv. U.S.* **69**, 253–266.

JOHNSTON, I. A. AND BRILL, R. W. (1984). Thermal dependence of contractile properties of single skinned muscle fibers from the Antarctic and various warm water marine fishes including skipjack tuna (*Katsuwonus pelamis*) and kawakawa (*Euthynnus affinis*). *J. comp. Physiol.* **155**, 63–70.

KISHINOUYE, K. (1923). Contributions to the comparative study of the so-called scombroid fishes. *J. Coll. Agric. imp. Univ. Tokyo* **8**, 293–475.

LIGHTHILL, M. J. (1975). *Mathematical Biofluiddynamics*. Philadelphia: SIAM.

LIGHTHILL, M. J. (1977). Mathematical theories of fish swimming. In *Fisheries Mathematics* (ed. J. H. Steel), pp. 131–144. New York: Academic Press.

LINDSEY, C. C. (1978). Form, function and locomotory habits in fish. In *Fish Physiology*, vol. VII (ed. W. S. Hoar and D. J. Randall), pp. 1–100. New York: Academic Press.

MAGNUSON, J. J. (1970). Hydrostatic equilibrium of *Euthynnus affinis*, a pelagic teleost without a swim bladder. *Copeia* **1970**, 56–85.

MAGNUSON, J. J. (1973). Comparative study of adaptations for continuous swimming and hydrostatic equilibrium of scombroid and xiphoid fishes. *Fishery Bull. Fish Wildl. Serv. U.S.* **71**, 337–356.

MAGNUSON, J. J. (1978). Locomotion by scombrid fishes: Hydromechanics, morphology and behavior.

In *Fish Physiology*, vol. VII (ed. W. S. Hoar and D. J. Randall), pp. 240–315. New York: Academic Press.

NURSALL, J. R. (1956). The lateral musculature and the swimming of fish. *Proc. zool. Soc. Lond.* **126**, 127–143.

STEVENS, E. D. AND FRY, F. E. J. (1971). Brain and muscle temperatures in ocean caught and captive skipjack tuna. *Comp. Biochem. Physiol.* **38**A, 203–211.

WARDLE, C. S. (1975). Limit of fish swimming speed. *Nature* **255**, 725–727.

WARDLE, C. S. AND HE, P. (1988). Burst swimming speeds of mackerel, *Scomber scomber* L. *J. Fish Biol.* **32**, 471–478.

WARDLE, C. S. AND VIDELER, J. J. (1980). How do fish break the speed limit? *Nature* **284**, 445–447.

WARDLE, C. S., VIDELER, J. J., ARIMOTO, T., FRANCO, J. M. AND HE, P. (1989). The muscle twitch and the maximum swimming speed of giant bluefin tuna, *Thunnus thynnus*, L. *J. Fish Biol.* **35**, 129–137.

WEBB, P. W. (1975). Hydrodynamics and energetics of fish propulsion. *Bull. Fish. Res. Bd Can.* **190** 1-158.

WEBB, P. W. (1988). 'Steady' swimming kinematics of tiger musky, an esociform accelerator and rainbow trout, a generalist cruiser. *J. exp. Biol.* **138**, 51–69.

WEBB, P. W. (1992). The high cost of body/caudal fin undulatory swimming due to increased friction drag or inertial recoil. *J. exp. Biol.* **162**, 157–166.

WEBB, P. W., KOSTECKI, P. T. AND STEVENS, E. D. (1984). The effect of size and swimming speed on locomotory kinematics of rainbow trout. *J. exp. Biol.* **109**, 77–95.

WU, T. Y. AND YATES, G. T. (1978). A comparative mechanophysiological study of fish locomotion with implications for tuna-like swimming mode. In *The Physiological Ecology of Tunas* (ed. G. D. Sharp and A. E. Dizon), pp. 313–337. New York: Academic Press.

YUEN, H. S. H. (1966). Swimming speeds of yellowfin and skipjack tuna. *Am. Fish. Soc. Trans.* **95**, 203–208.